

Research Paper

Resveratrol as a new inhibitor of immunoproteasome prevents PTEN degradation and attenuates cardiac hypertrophy after pressure overload

Chen Chen^{a,1}, Lei-Xin Zou^{a,1}, Qiu-Yue Lin^b, Xiao Yan^a, Hai-Lian Bi^b, Xin Xie^b, Shuai Wang^c, Qing-Shan Wang^a, Yun-Long Zhang^{a,b,*}, Hui-Hua Li^{a,b,*}

^a Department of Nutrition and Food Hygiene, School of Public Health, Dalian Medical University, Dalian 116044, China

^b Department of Cardiology, Institute of Cardiovascular Diseases, First Affiliated Hospital of Dalian Medical University, Dalian 116011, China

^c Department of Ophthalmology, Second Affiliated Hospital of Dalian Medical University, Dalian 116023, China



ARTICLE INFO

Keywords:

Resveratrol
Cardiac hypertrophy
Immunoproteasome
PTEN degradation
AKT/mTOR
AMPK

ABSTRACT

Sustained cardiac hypertrophy is a major cause of heart failure (HF) and death. Recent studies have demonstrated that resveratrol (RES) exerts a protective role in hypertrophic diseases. However, the molecular mechanisms involved are not fully elucidated. In this study, cardiac hypertrophic remodeling in mice were established by pressure overload induced by transverse aortic constriction (TAC). Cardiac function was evaluated by echocardiography and invasive pressure-volume analysis. Cardiomyocyte size was detected by wheat germ agglutinin staining. The protein and gene expressions of signaling mediators and hypertrophic markers were examined. Our results showed that administration of RES significantly suppressed pressure overload-induced cardiac hypertrophy, fibrosis and apoptosis and improved in vivo heart function in mice. RES also reversed pre-established hypertrophy and restoring contractile dysfunction induced by chronic pressure overload. Moreover, RES treatment blocked TAC-induced increase of immunoproteasome activity and catalytic subunit expression ($\beta 1i$, $\beta 2i$ and $\beta 5i$), which inhibited PTEN degradation thereby leading to inactivation of AKT/mTOR and activation of AMPK signals. Further, blocking PTEN by the specific inhibitor VO-Ohipc significantly attenuated RES inhibitory effect on cardiomyocyte hypertrophy in vivo and in vitro. Taken together, our data suggest that RES is a novel inhibitor of immunoproteasome activity, and may represent a promising therapeutic agent for the treatment of hypertrophic diseases.

1. Introduction

Pathological cardiac hypertrophy is associated with significantly increased risk of heart failure (HF), one of the leading medical causes of mortality worldwide. Cardiomyocyte hypertrophy is characterized by increased cell size, protein synthesis and activation of fetal gene expression, which are regulated by protein kinase signaling cascades [1,2]. In addition to gene transcription, enhanced protein synthesis is an important cellular process during hypertrophy. The master regulator of protein synthesis in the cardiac myocyte is PI3K/AKT/mTOR pathway, and AKT is the central mediator of this pathway with multiple downstream effectors that contribute to cardiac hypertrophy [3–5]. While AMP-activated protein kinase (AMPK) is a major regulator of cellular energy metabolism, which acts opposite to AKT, and is a negative regulator of the mTOR pathway and inhibit cardiac hypertrophy

[6]. Importantly, these signaling pathways are negatively modulated by a phosphatase PTEN (phosphatase and TENsin homologue deleted from chromosome 10) [7,8]. Interestingly, PTEN stability is also regulated by the ubiquitin-proteasome system (UPS) [9]. However, the regulatory mechanism for PTEN in cardiac hypertrophy remains elusive.

The ubiquitin-proteasome system (UPS) plays the major role in protein quality control in eukaryotic cells. The 20S proteasome has 3 standard catalytic subunits, namely $\beta 1$ (PSMB6), $\beta 2$ (PSMB7), and $\beta 5$ (PSMB5), which perform distinct proteolytic activities, including caspase-like, trypsin-like, and chymotrypsin-like. After stimulation of cytokine IFN- γ , the standard subunits can be replaced with the inducible subunits, such as $\beta 1i$ (PSMB9 or LMP2), $\beta 2i$ (PSMB10, LMP10 or MECL), and $\beta 5i$ (PSMB8 or LMP7), which form the core of the immunoproteasome [10]. The immunoproteasome has been implicated in controlling immune responses, oxidative stress, cell growth and

* Corresponding authors at: Department of Cardiology, Institute of Cardiovascular Diseases, First Affiliated Hospital of Dalian Medical University, Dalian 116011, China.

E-mail addresses: 674250228@qq.com (Y.-L. Zhang), hhl1935@aliyun.com (H.-H. Li).

¹ These authors contributed equally to this work.

<https://doi.org/10.1016/j.redox.2018.10.021>

Received 11 October 2018; Accepted 28 October 2018

Available online 01 November 2018

2213-2317/© 2018 The Authors. Published by Elsevier B.V. This is an open access article under the CC BY-NC-ND license (<http://creativecommons.org/licenses/by-nc-nd/4.0/>).

maintaining cellular protein homeostasis [10]. We recently reported that knockout of immunosubunit $\beta 2i$ reduced hypertension and cardiac fibrosis in DOCA (deoxycortone acetate)/salt mouse model [11]. Furthermore, $\beta 2i$ deletion attenuated Ang II-induced atrial inflammation, vascular permeability, fibrosis and atrial fibrillation [12,13]. These results suggest that immunoproteasome plays a role in cardiac diseases, and strategies aimed at inhibiting immunoproteasome activity may offer novel and effective therapeutic approaches to prevent these diseases.

Resveratrol (3,5,4'-trihydroxystilbene, RES or RSV) is a polyphenol compound that is found in more than 70 plant species. Early studies have shown that RES has antioxidative, anticancer and antibacterial effects in many pathological conditions [14]. Increasing evidence suggests that RES exerts cardioprotective effects against myocardial ischemia/reperfusion and myocardial infarction through increasing antioxidant efficacy and upregulation of NO production, antagonizing fractalkine or enhancing VEGF-mediated angiogenesis [15–18]. Moreover, RES reduces hypertension and subsequent cardiac hypertrophy in mice induced by various hypertrophic stimuli such as pressure overload, Ang II or deoxycorticosterone acetate (DOCA)-salt. These effects are associated with increasing NO, AMPK activation, lowering oxidative stress, Ang II and ET-1 [18–21]. Moreover, RES also prevents cardiac hypertrophy and HF through regulating LKB1/AMPK and p70S6 kinase signaling pathways in hypertensive rats [22,23]. However, the molecular mechanisms by which RES regulates these signaling pathways and attenuates pressure overload-induced cardiac hypertrophic remodeling remain to be elucidated.

In this study, we demonstrated that administration of RES significantly prevents and reverses pressure overload-induced cardiac hypertrophic remodeling and dysfunction in mice. The beneficial effect was associated with inhibition of immunoproteasome catalytic subunit expression and activities, which reduces PTEN degradation leading to inhibition of AKT/mTOR and activation of AMPK signaling pathways. Taken together, these results identify that RES is a new inhibitor of immunoproteasome activity, and could be a promising agent for treating cardiac hypertrophic diseases.

2. Material and methods

2.1. Animals, transverse aortic constriction operation and treatment

Male wild-type (WT) C57BL/6 mice were purchased from Jackson Laboratory (Bar Harbor, ME, USA). The investigation was approved by the Animal Care and Use Committee of Dalian Medical University and conformed to the Guide for the Care and Use of Laboratory Animals published by the U.S. National Institutes of Health (NIH Publication No. 85-23, revised 1996). Pressure overload-induced hypertrophic model was induced by transverse aortic constriction (TAC) as described previously [24]. Briefly, WT mice (8-week-old) were anesthetized with isoflurane. The left chest of mice was opened. A 7.0 nylon suture ligature was tied against a 27-gauge needle at the transverse aorta to produce a 65–70% constriction after removal of the needle. Adequate aortic constriction was induced and confirmed by Doppler analysis. Sham operation was performed with a similar procedure without ligation. All surgeries and subsequent analyses were conducted in a blinded manner.

All mice ($n = 40$) were randomly allocated to 4 groups: Sham, TAC, TAC+RES (25 mg/kg body weight (BW)) and TAC+RES (50 mg/kg BW). Animals were subjected to TAC operation and orally gavaged with RES at doses of 25 and 50 mg/kg BW daily in the presence or absence of VO-OHPic (10 mg/kg), a specific PTEN inhibitor. After 2 or 4 weeks of sham or TAC operation mice were anesthetized with an overdose of pentobarbital (100 mg/kg, Sigma-Aldrich). The hearts were removed and prepared for further histological and molecular analysis. All investigations were approved by the Animal Care and Use Committee of Dalian Medical University and conformed to the US National Institutes

of Health Guide for the Care and Use of Laboratory and the ARRIVE guidelines [25].

2.2. Antibodies and reagents

Antibodies against PTEN (#9188), p-mTOR (#5536), m-TOR (#2972), p-AKT (#9271), AKT (#9272), p-ERK1/2 (#4370), ERK1/2 (#4695), p-STAT3 (#9131), STAT3 (#8768), p-AMPK α (#50081), AMPK α (#2532), GAPDH (#2118) and horseradish peroxidase-linked anti-mouse or anti-rabbit IgG (#7074) were purchased from Cell Signaling Technology (Boston, USA). Anti- $\beta 1i$ (ab190350), $\beta 2i$ (ab183506), and $\beta 5i$ (ab3329) were purchased from Abcam (London, England). p-S6K (om267088), S6K (om267092) were purchased from OmnimAbs (Alhambra, CA, USA). Bax (50599-2-Ig), Bcl-2 (66799-1-Ig), and caspase-3 (66470-2-Ig) were purchased from Proteintech Group (Rosemont, USA). MitoTracker Red CMXRos (M7512) was purchased from Invitrogen (Carlsbad, CA, USA). VO-OHPic trihydrate was purchased from MedChem Express (Monmouth Junction, NJ, USA). Primers including atrial natriuretic peptide (ANF) and brain natriuretic peptide (BNP) were purchased from Sangon Biotech (Shanghai, China). RES was purchased from Selleck (Houston, TX, USA). VO was purchased from Med Chem Express (Ann Arbor, MI, USA). Wheat germ agglutinin (WGA) and Anti-ubiquitin (#U5379) were purchased from Sigma-Aldrich (St Louis, MO, USA). TRizol was obtained from Invitrogen (Carlsbad, CA). All other chemicals frequently used in our laboratory were purchased from Sigma-Aldrich.

2.3. Echocardiography

Transthoracic echocardiography was performed on mice at indicated time points after TAC operation by a 30 MHz probe (Vevo 1100 system; VisualSonics, Toronto, Ontario, Canada) as previously described [26–28]. The left ventricular internal dimension (LVID) at diastole and systole, LV posterior wall thickness (LVPW) at diastole and systole, LV ejection fraction (EF%) and LV fractional shortening (FS%) were calculated.

2.4. Histopathological analysis

The heart tissues were fixed in 4% paraformaldehyde solution for 24 h, then embedded in paraffin and sectioned (5 μ m). Hematoxylin and eosin (H&E) staining was performed on the heart sections according to standard procedure [26,28]. Masson's trichrome staining was performed to examine collagen deposition [27,28]. To evaluate myocyte cross-sectional area, heart sections were stained with 50 μ g/mL of rhodamine-labeled wheat germ agglutinin (WGA) for 60 min. Digital images were taken at $\times 100$ or $\times 200$ magnification of over 20 random fields from each heart sample. Each cell area was calculated by measuring 15–200 cells per sample. In order to detect apoptotic death in heart tissues, terminal-deoxynucleotidyl transferase-mediated UTP nick end labeling (TUNEL) assay was carried out following the manufacturer's instruction (Roche Diagnostics, IL, USA). After TUNEL staining, cells were counter-stained with DAPI before mounting. Generally, cells with nuclear staining were considered to be apoptotic. The images were analyzed using Image Pro Plus 3.0 (Nikon, Tokyo, Japan).

2.5. Culture of primary cardiomyocytes

Neonatal rat cardiac myocytes (NRCMs) were obtained from Sprague-Dawley rats (1–3 days) as described previously [12,24]. Briefly, hearts cut into about 1 mm³ and then dissociated with 0.04% trypsin and 0.07% collagenase II. Cells were dispersed and plated on 100-mm dishes in 5% CO₂ at 37 °C for 1.5 h. Suspended cardiomyocytes were collected and transferred into 6- or 24-well plates with coating laminin (10 μ g/mL). Cardiomyocytes were cultured in DMEM/F12 supplemented with 10% FBS for 16–20 h and then replaced with serum-

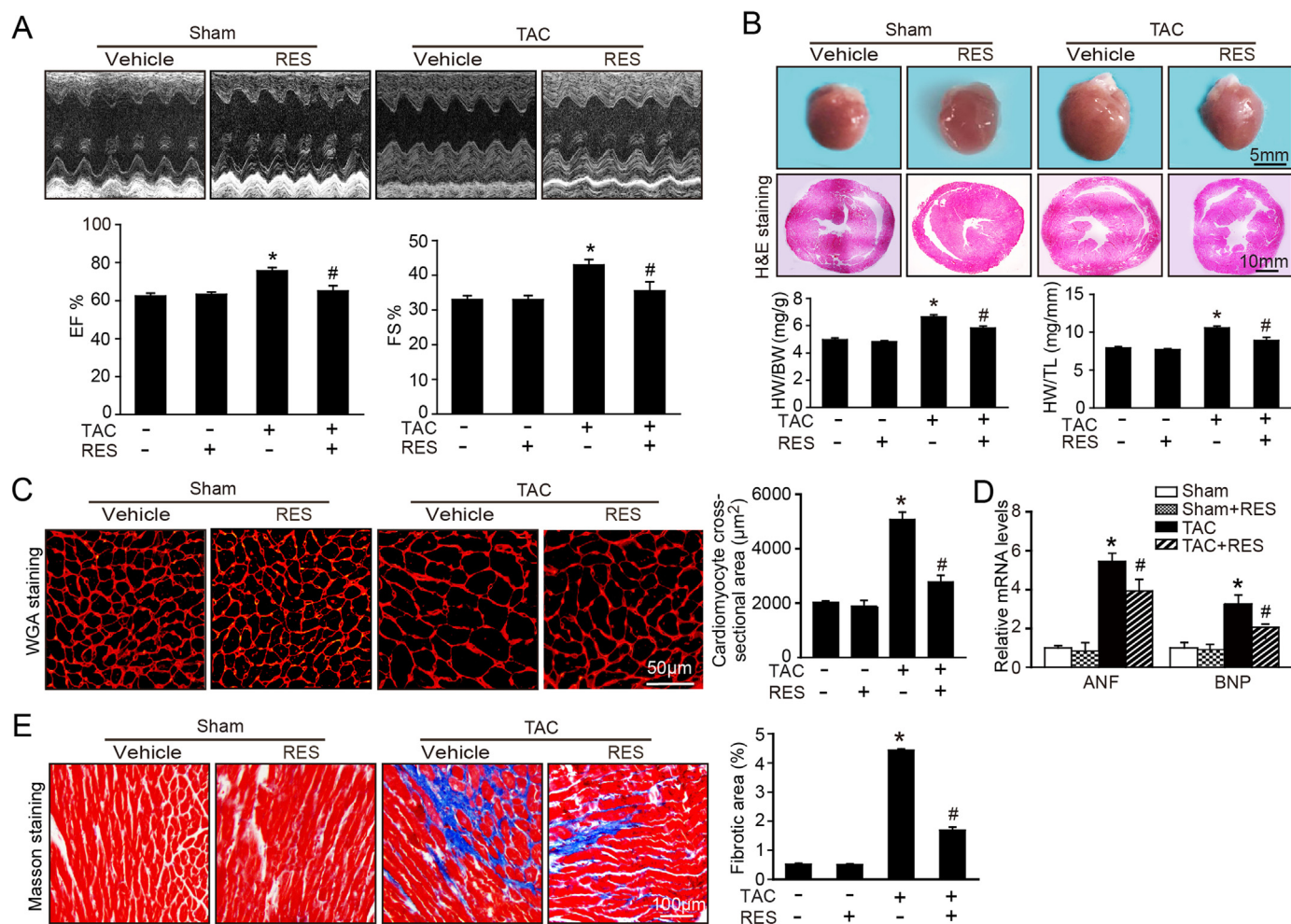


Fig. 1. Resveratrol (RES) ameliorates pressure overload-induced cardiac hypertrophy and dysfunction in vivo. **A**, Representative M-mode echocardiography of left ventricular chamber (upper), and measurement of left ventricular ejection fraction (EF%) and fractional shortening (FS%) (lower, $n = 10$). **B**, Representative gross images of whole hearts (upper). Scale bar: 5 mm. Representative images of H&E staining (middle). Scale bar: 10 mm. The ratios of heart weight to body weight (HW/BW) and heart weight tibial length (HW/TL) ($n = 10$; lower). **C**, Representative images of TRITC-labeled wheat germ agglutinin (WGA) staining to detect cardiac hypertrophy (left). Scale bar: 50 μm . Quantification of the relative myocyte cross-sectional area ($n = 8$, 200 cells counted per heart; right). **D**, qPCR analyses of ANF and BNP mRNA levels. **E**, Representative images of Masson's trichrome staining (left) and quantification of fibrotic area (right, $n = 8$). Scale bar: 100 μm . The results are normalized to the GAPDH content. Data are presented as mean \pm SEM, and n represents number of animals, * $P < 0.05$ versus Sham, # $P < 0.05$ versus TAC+RES.

free medium for 12 h before experiments.

2.6. Measurement of proteasome activity

Measurement of proteasome activity in the hearts was performed using fluorogenic peptide substrates, including caspase-like activity with Z-LLE-AMC (45 $\mu\text{mol/L}$), trypsin-like activity with Ac-RLR-AMC (40 $\mu\text{mol/L}$), and chymotrypsin-like activity with Suc-LLVY-AMC (18 $\mu\text{mol/L}$) as described [12,13,23,29].

2.7. Real-time PCR analysis

Quantitative real-time PCR (qPCR) was performed with an iCycler IQ system (Bio-Rad, CA) as described previously [26,28]. Total RNA from left ventricle was extracted with TRIzol (Invitrogen) and reverse-transcribed. cDNA (1–2 μg) was used for PCR amplification with gene-specific primers, including ANF and BNP. Transcript quantities were compared by using the relative quantitative method, where the amount of detected mRNA normalized to the amount of endogenous control (GAPDH).

2.8. Western blot analysis

Proteins were extracted from snap-frozen heart tissue using RIPA buffer (Solarbio Science Technology Co., Beijing, China). The protein lysates were separated by electrophoresis in 8–12% SDS-PAGE gels and transferred to polyvinylidene difluoride (PVDF) membranes. The membranes were incubated with the appropriate antibodies at 4 $^{\circ}\text{C}$ overnight, and then with horseradish peroxidase-conjugated secondary antibodies (1:5000) for 1 h at room temperature. All blots were developed by using the ECL Plus chemiluminescent system, and signal intensities were analyzed with a Gel-pro 4.5 Analyzer (Media Cybernetics, USA) [24,30–32].

2.9. NAD/NADH assay

Intracellular NAD and NADH levels were detected by NAD/NADH Assay Kit (Abcam, London, England) according to manufacturer's instructions. Briefly, 2×10^5 cells were washed with cold PBS and then lysed with NADH/NAD Extraction Buffer at room temperature. Total NAD and NADH levels were analyzed following the instruction in a 96-well plate and color were developed and read at 450 nm. The

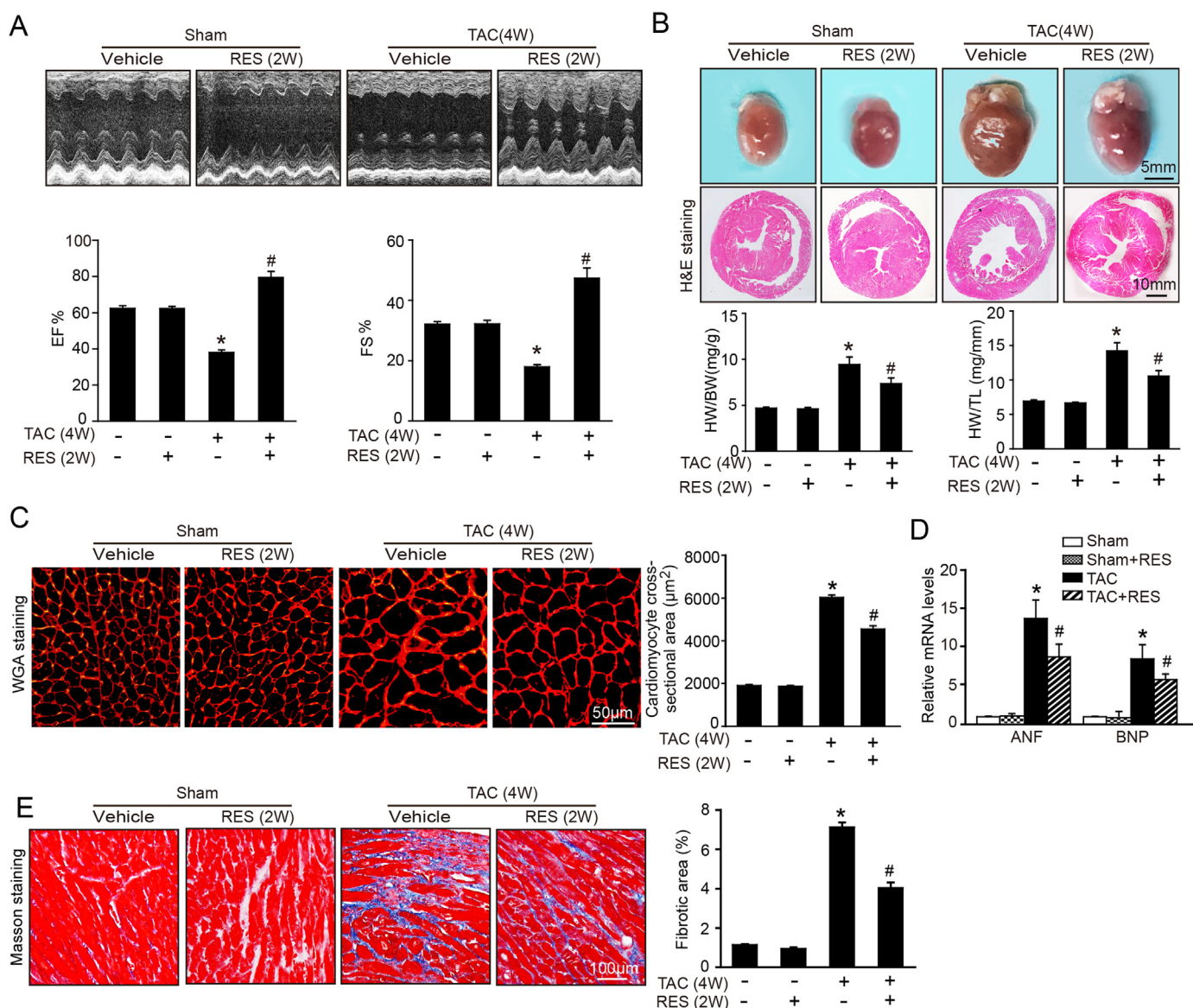


Fig. 2. RES reverses preestablished cardiac hypertrophy and dysfunction in vivo. A, Representative M-mode echocardiography of left ventricular chamber (upper), and assessment of left ventricular EF% and FS% (lower, n = 10). B, Representative gross images of whole hearts (upper). Scale bar: 5 mm. Representative images of H & E staining (middle). Scale bar: 10 mm. The ratios of HW/BW and HW/TL (n = 10; lower). C, Representative images of TRITC-labeled WGA to detect cardiac hypertrophy (left). Scale bar: 50 µm. Quantification of the relative myocyte cross-sectional area (n = 8, 200 cells counted per heart; right). D, qPCR analyses of ANF and BNP mRNA levels. E, Representative images of Masson's trichrome staining (left) and quantification of fibrotic area (right, n = 8). Scale bar: 100 µm. The data are normalized to the GAPDH content. Data are presented as mean ± SEM, and n represents number of animals, *P < 0.05 versus sham group, #P < 0.05 versus TAC+RES.

concentration of total NAD and NADH were expressed in pmol/10⁶ cells. NAD/NADH ratio is calculated as: [NAD-NADH]/NADH.

2.10. Statistical analysis

The results are expressed as mean ± standard error of the mean (SEM). The unpaired 2-tailed t-test was utilized to compare the 2 groups. The significance of difference between the means of groups was statistically compared using one-way ANOVA by Newman-Keuls multiple comparison test with GraphPad Prism 5 (GraphPad Prism Software). The values of P < 0.05 were considered statistically significant.

3. Results

3.1. RES ameliorates pressure overload-induced cardiac hypertrophy and dysfunction

To determine the effect of RES on the cardiac hypertrophy and contractile function in vivo, WT mice were injected into with vehicle or RES at dose of 25 or 50 mg/kg daily and subjected to sham or TAC surgery for 2 weeks. Echocardiography assessment showed that TAC-induced enhancement of left ventricular contractile function as indicated by the increased EF% and FS% was markedly reversed by RES (50 mg/kg BW) in TAC-treated mice (Fig. 1A). Moreover, after 2 weeks of TAC, WT mice exhibited a marked chamber and myocyte hypertrophy as indicated by increased heart size, LV wall thickness and heart weight/body weight (HW/BW) and heart weight/tibia length (HW/TL) ratios compared with sham control, whereas these changes were

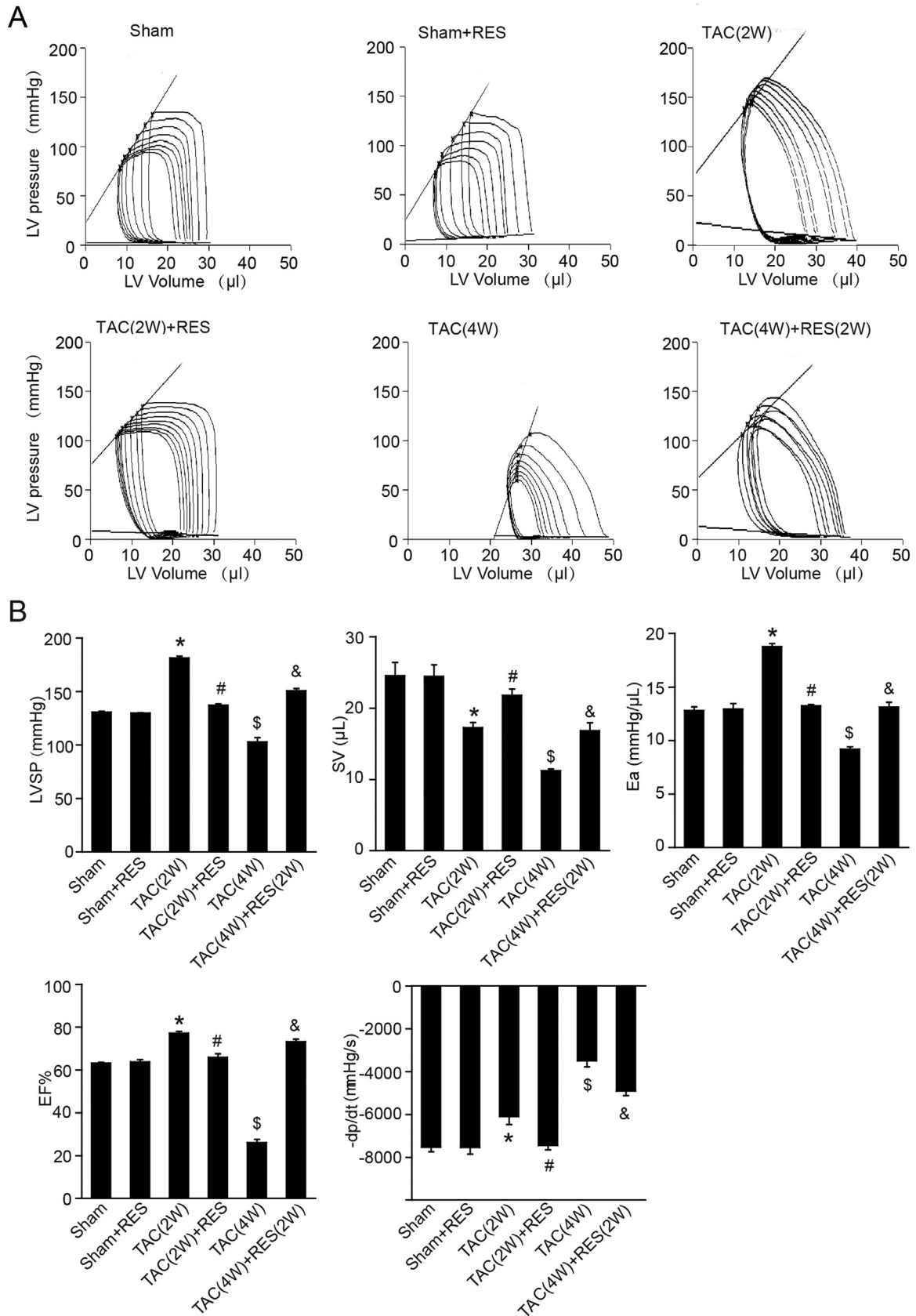


Fig. 3. Pressure-volume analysis of systolic and diastolic function. A, Representative left-ventricular pressure-volume loops in each group. B, Summary data on systolic function and diastolic function. LVSP, left ventricle systolic pressure. SV, stroke volume. Ea, arterial elastance (measure of ventricular afterload). EF, ejection fraction. $-dp/dt$, maximal rate of pressure decline (diastolic indexes). Data are presented as mean \pm SEM, and n represents number of animals. * $P < 0.05$ versus sham; # $P < 0.05$ versus TAC (2W); \$ $P < 0.05$ versus sham; & $P < 0.05$ versus TAC (4W).

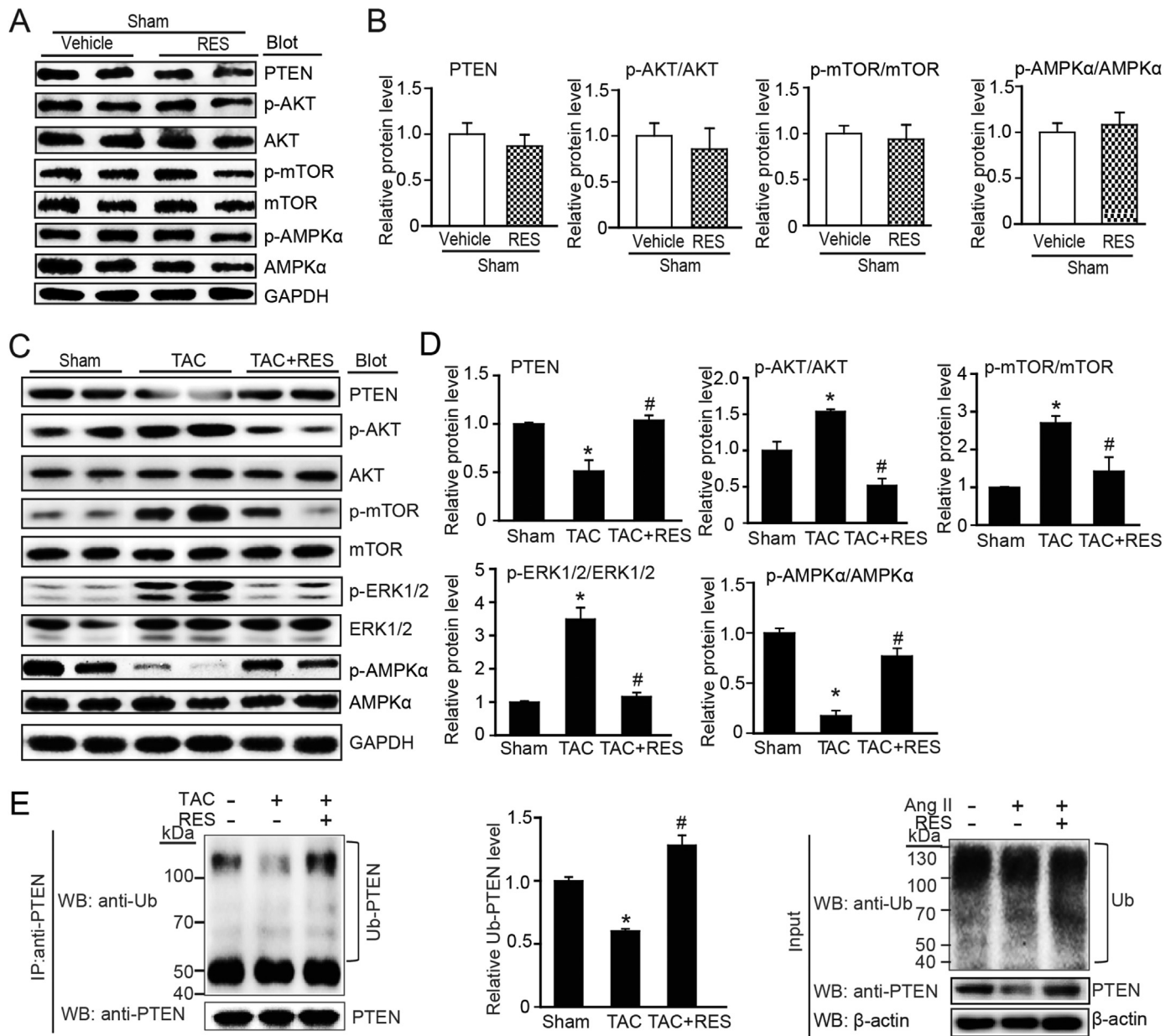


Fig. 4. RES attenuates pressure overload-induced activation of ATK/mTOR, inactivation of AMPK and degradation of PTEN in the heart after TAC operation. **A**, Representative immunoblotting analyses of PTEN, p-AKT, AKT, p-mTOR, mTOR, p-AMPK and AMPK in the heart after sham operation. **B**, Quantification of the relative protein levels ($n = 4$). **C**, Representative immunoblotting analyses of PTEN, p-AKT, AKT, p-mTOR, mTOR, p-AMPK α and AMPK α in the heart after TAC operation with or without RES treatment (left). **D**, Quantification of the relative protein levels ($n = 4$). GAPDH as an internal control. **E**, Lysates from heart tissues treated with TAC or sham in the presence or absence of RES before harvest were immunoprecipitated with anti-PTEN. The ubiquitin-conjugated PTEN was detected by immunoblotting with anti-ubiquitin (Ub, upper) and anti-PTEN (lower). Quantification of the relative Ub-PTEN level (middle). Input showed the expression of corresponding proteins in whole cell lysates (right).

attenuated by RES (50 mg/kg BW) in TAC-treated mice (Fig. 1B–C). Since ventricular myocyte enlargement and fibrosis are hallmarks of cardiac hypertrophic remodeling, we then examined the effect of RES on LV cardiomyocyte size and collagen deposition. After 2 weeks of TAC, WT mice showed an increase in the cross-sectional areas of myocytes, fibrotic area and the mRNA expression of hypertrophic markers (ANP and BNP) compared with sham control, and this effect was markedly reduced by RES (50 mg/kg BW) in TAC-treated mice (Fig. 1D–E). In addition, the number of TUNEL-positive nuclei, Bax/Bcl-2 ratio and cleaved caspase-3 level were also lower in RES-treated mice than that in vehicle control after TAC operation (Supplemental Fig. 1A–C). Interestingly, treatment of mice with RES at low dose (25 mg/kg BW) had no significant effect on TAC-induced cardiac

hypertrophy and dysfunction. RES treatment had no significant effect on cardiac function, hypertrophic remodeling and myocyte apoptosis compared with vehicle-treated control after sham operation (Fig. 1A–E, Supplemental Fig. 1A–C). Overall, these results indicate that RES improves TAC-induced compensatory cardiac hypertrophic remodeling and dysfunction.

3.2. RES reverses preestablished cardiac hypertrophy and dysfunction

To assess whether RES reverses the preestablished cardiac hypertrophy, WT mice were subjected to TAC operation for 2 weeks, and then intravenously injected with RES (50 mg/kg BW) or vehicle only for an additional 2 weeks. Administration of RES significantly restored TAC-

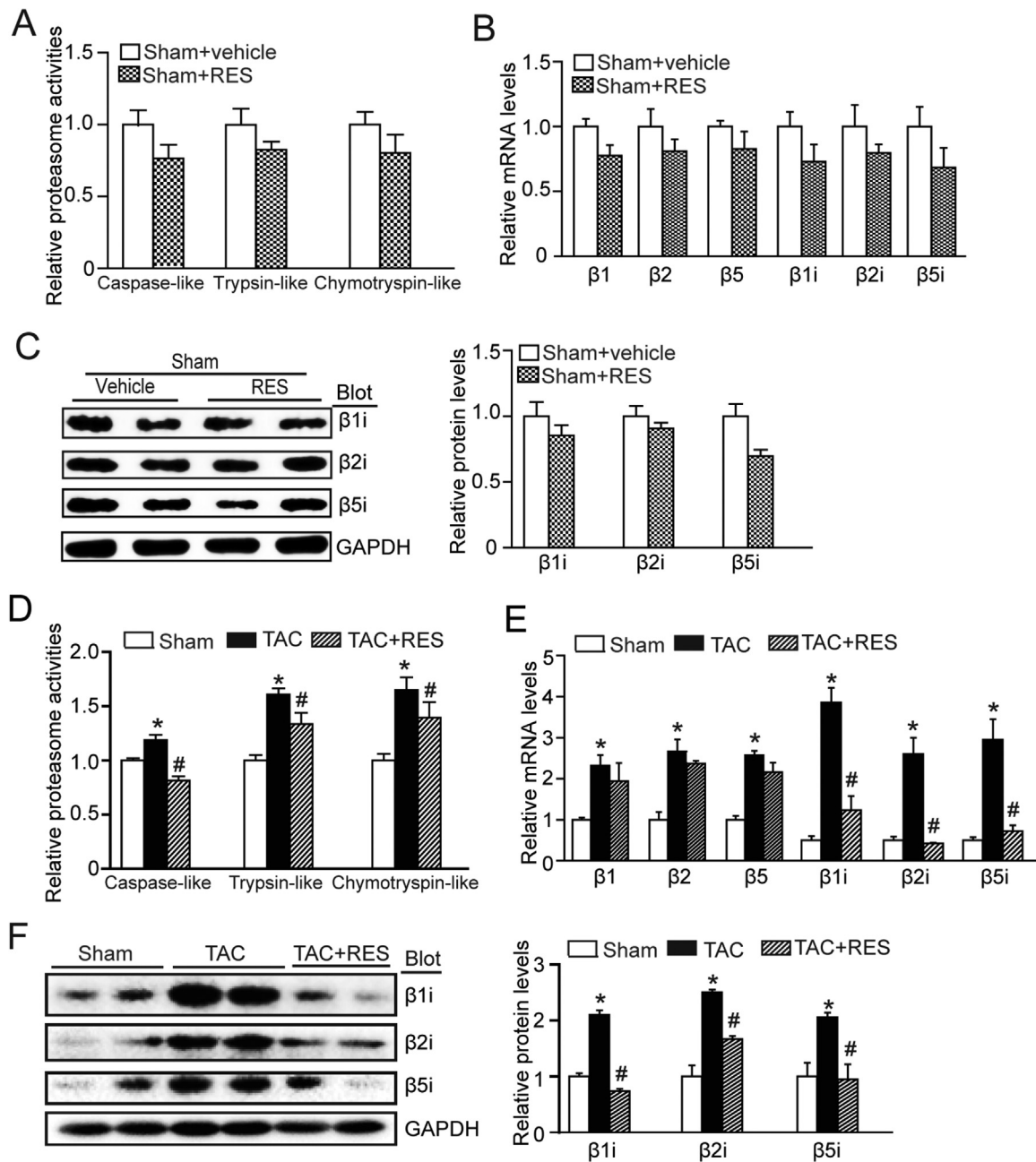


Fig. 5. RES reduces immunoproteasome activity and catalytic subunit expression in the heart after TAC operation. **A**, The proteasome activities including caspase-like, trypsin-like, and chymotrypsin-like activities were measured in the heart after sham operation. Activities are indicated as percentages of those in sham group. **B**, qPCR analyses of catalytic subunit ($\beta 1$, $\beta 2$, $\beta 5$, $\beta 1i$, $\beta 2i$, and $\beta 5i$) mRNA levels ($n = 4$). **C**, Representative immunoblotting analyses of $\beta 1i$, $\beta 2i$, and $\beta 5i$ protein levels (left), and quantification of the relative protein levels (right, $n = 4$). **D**, The proteasome activities were measured in the heart after TAC operation with or without RES treatment ($n = 4$). **E**, qPCR analyses of $\beta 1$, $\beta 2$, $\beta 5$, $\beta 1i$, $\beta 2i$, and $\beta 5i$ mRNA levels. **F**, Representative immunoblotting analyses of $\beta 1i$, $\beta 2i$, and $\beta 5i$ protein levels (left), and quantification of the relative protein levels (right, $n = 4$). GAPDH as an internal control. * $P < 0.05$ versus sham group, # $P < 0.05$ versus TAC + RES.

induced decrease of cardiac contractile function as evidenced by the EF % and FS% compared with vehicle treatment after total 4 weeks of TAC (Fig. 2A). Furthermore, TAC-induced hypertrophic remodeling as indicated by increased heart size, chamber dilation, HW/BW and HW/TL ratios, myocyte cross-sectional areas, fibrotic area and the mRNA expression of ANF and BNP were all markedly attenuated in RES-treated mice (Fig. 2B–E). There was no significant difference in cardiac function and hypertrophic remodeling between RES- and vehicle-treated groups after sham operation (Fig. 2A–E). These results indicate that RES is effective to reverse the transition from compensatory hypertrophy to HF.

3.3. RES improves cardiac function in vivo

To further examine the protective effect of RES on cardiac function in vivo, we performed invasive pressure-volume analysis before and during transient reduction of chamber preload to generate specific end-systolic and end-diastolic pressure volume relations. TAC operation for 2 weeks led to rightward shift of the loops and end-systolic pressure-volume relation associated with enhanced left ventricle systolic pressure (LVSP), arterial elastance (Ea; an index of total ventricular afterload) and ejection fraction (EF), reduced stroke volume (SV) and maximal rate of pressure decline ($-dP/dt$) compared with sham controls consistent with hypertrophy remodeling, and this effect was

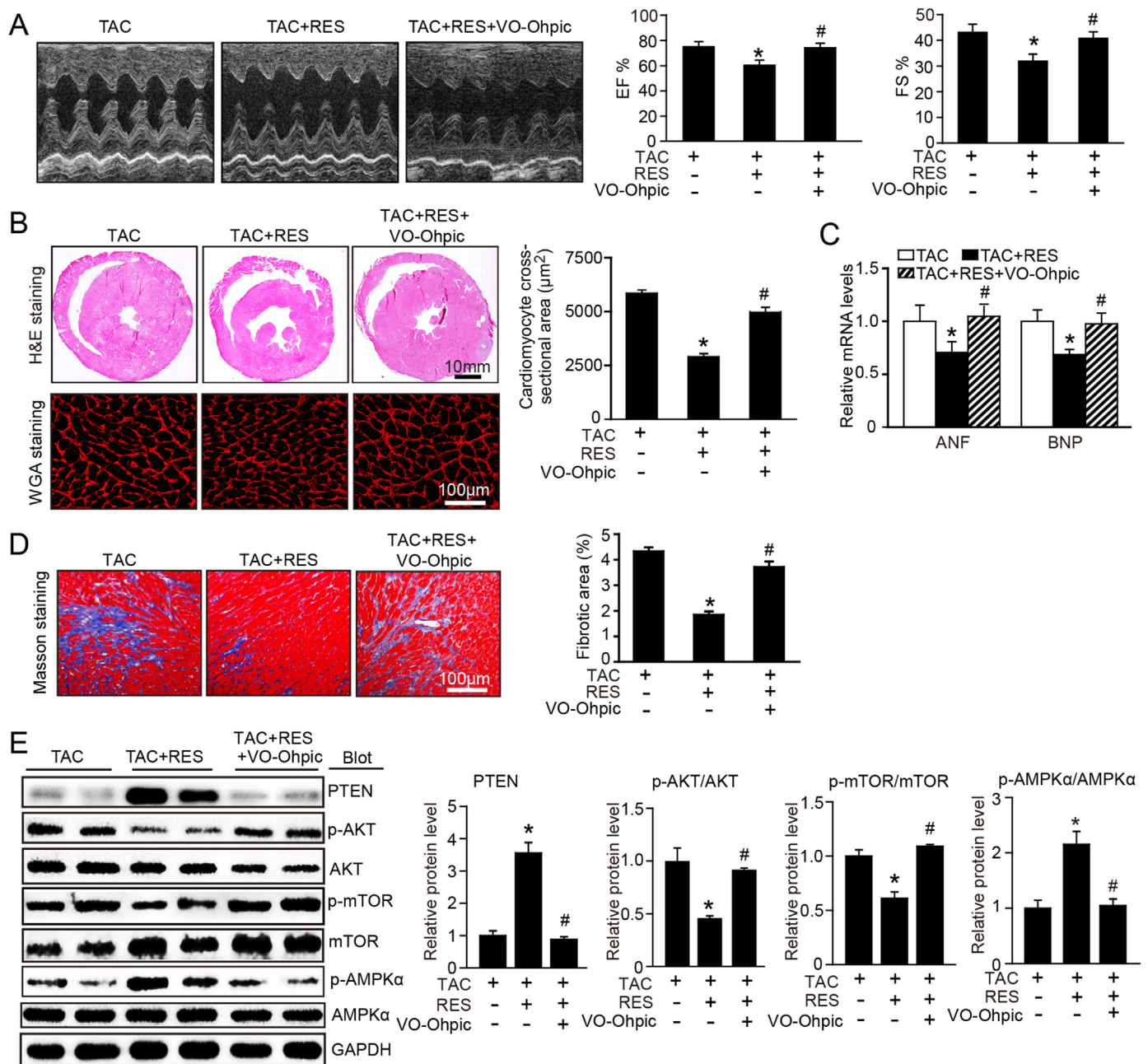


Fig. 6. Blocking of PTEN activity suppresses RES-mediated inhibitory effect on cardiac hypertrophy. **A**, Representative M-mode echocardiography of left ventricular chamber (left), and measurement of left ventricular EF% and FS% in mice after TAC in the presence or absence of RES (50 mg/kg BW) together with VO-ohpic (10 mg/kg BW) (right, n = 8). **B**, Representative images of H&E staining (upper), TRITC-labeled WGA staining (middle) and Masson's trichrome staining (lower). Quantification of the relative myocyte cross-sectional area (n = 8, 200 cells counted per heart) and fibrotic area (right, n = 8). **C**, qPCR analyses of ANF and BNP mRNA levels. **D**, Representative immunoblotting analyses of PTEN, p-AKT, AKT, p-mTOR, mTOR, p-AMPKα and AMPKα in the heart (left). Quantification of the relative protein levels (right, n = 4). GAPDH as an internal control. *P < 0.05 versus TAC, #P < 0.05 versus TAC+RES.

reversed by RES treatment (2W) (Fig. 3A–B). Moreover, TAC for 4 weeks triggered the progression of cardiac dysfunction, as indicated by a decrease in LVSP, SV, Ea, EF and -dp/dt associated with a rightward shift of pressure-volume relation, and a decrease in the slope of end systolic pressure-volume relation in WT mice, which were also improved when RES was administered for additional 2 weeks after hypertrophy was already established (TAC-4W+RES-2W) (Fig. 3A–B). RES treatment had no significant effect on these parameters compared with vehicle treatment after sham operation (Fig. 3A–B).

3.4. RES attenuates PTEN degradation and activation of ATK/mTOR signaling but induces AMPK activation in the heart after pressure overload

To elucidate the molecular mechanisms whereby RES ameliorate TAC-induced cardiac hypertrophy and dysfunction, we evaluated multiple signaling pathways that play critical role in this process. RES treatment had no significant effect on the main signaling mediators such as AKT, mTOR and AMPK compared with vehicle treatment after sham operation (Fig. 4A–B). TAC operation for 2 weeks markedly induced activation of AKT, mTOR, S6K, and ERK1/2 and inhibition of AMPK activation compared with sham controls, but this effect was reversed by RES in TAC-treated mice (Fig. 4C–D). It is reported that

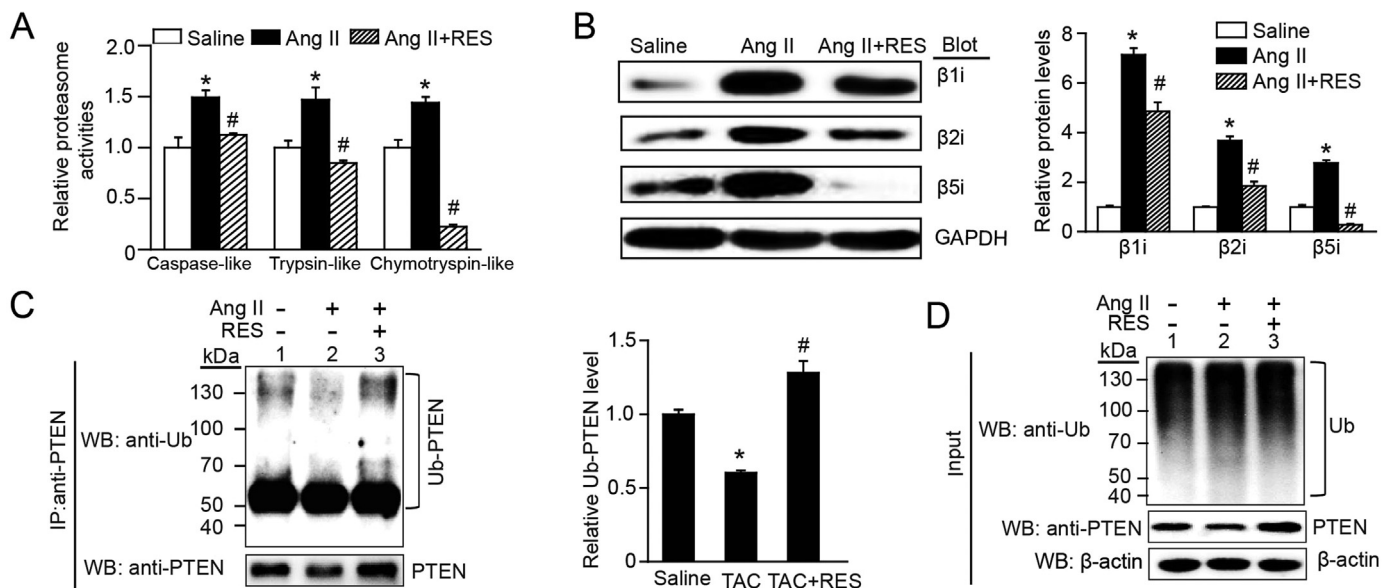


Fig. 7. RES inhibits immunoproteasome activity and PTEN degradation in vitro. **A**, The proteasome activities (caspase-like, trypsin-like and chymotrypsin-like) were measured in neonatal rat cardiomyocytes (NRCMs) treated with RES (100 μ M) or vehicle and stimulated with Ang II (100 nM) for 24 h (n = 6). **B**, Representative immunoblotting analyses of β 1i, β 2i and β 5i protein levels in NRCMs treated as in **A** (n = 3, left). Quantification of the relative protein levels (right). GAPDH as an internal control. **C**, Lysates from NRCMs treated with Ang II or saline in the presence or absence of RES before harvest were immunoprecipitated with anti-PTEN. The ubiquitin-conjugated PTEN was detected by immunoblotting with anti-ubiquitin (Ub, upper) and anti-PTEN (lower). Quantification of the relative Ub-PTEN level (right, n = 3). **D**, Input showed the expression of corresponding proteins (Ub and PTEN) in whole cell lysates (right).

activation of AKT and AMPK signals are regulated by PTEN [33], which is modulated by ubiquitin-proteasome system [9]. We then tested the effect of RES on PTEN protein stability and ubiquitination. Immunoblotting analysis showed that TAC-induced downregulation of PTEN protein, which was markedly reversed in RES-treated mice (Fig. 4C–D). Moreover, immunoprecipitation assay revealed that TAC-induced reduction of PTEN ubiquitination was also restored in RES-treated hearts (Fig. 4E). These results indicate that RES can suppress PTEN ubiquitination and degradation leading to inhibition of AKT signaling and activation of AMPK.

3.5. RES inhibits immunoproteasome activity and catalytic subunit expression in pressure overload hearts

To examine whether PTEN degradation is mediated by proteasome, we evaluated the action of RES on proteasome activities and catalytic subunit expression in the heart. RES treatment significantly blunted TAC-induced proteasome activities, including caspase-like, trypsin-like and chymotrypsin-like activities (Fig. 5A). Because three standard subunits (β 1, β 2 and β 5) and immonosubunits (β 1i, β 2i and β 5i) have the proteasome activity, we then examined their expression using qPCR analysis. Although RES treatment reduced proteasome activities (caspase-like, trypsin-like and chymotrypsin-like) and the mRNA levels of proteasome subunits (β 1, β 2, β 5, β 1i, β 2i and β 5i) compared with vehicle control, there was no statistically significant difference between two groups after sham operation (Fig. 5A–C). Moreover, RES significantly inhibited the mRNA levels of immonosubunits (β 1i, β 2i and β 5i) but not standard subunits (β 1, β 2 and β 5) in the hypertrophic hearts after TAC stress. Accordingly, TAC-induced upregulation of the protein levels of immonosubunits (β 1i, β 2i and β 5i) were also reduced in RES-treated heart tissues (Fig. 5D–F). Thus, these results suggest that RES prevents PTEN degradation likely through inhibiting immunoproteasome subunit expression and activities in TAC-induced hypertrophic heart.

3.6. Blocking of PTEN activity attenuates RES-mediated inhibitory effect on cardiac hypertrophy in mice

To further test whether PTEN is involved in TAC-induced cardiac hypertrophy and dysfunction after RES treatment, we treated mice with PTEN specific inhibitor VO-OHpic in the presence or absence of RES for 2 weeks. RES treatment markedly improved TAC-induced cardiac contractile dysfunction as indicated by increased FS% and EF% (Fig. 6A), attenuated cardiac cardiomyocyte hypertrophy, interstitial fibrosis and the mRNA expression of ANF and BNP, whereas these effects were reversed by VO-OHpic treatment (Fig. 6B–C). Correspondingly, RES treatment-induced upregulation of PTEN, inactivation of AKT/mTOR signaling and activation of AMPK were also reversed by VO-OHpic in RES-treated mice (Fig. 6D). Taken together, these results suggest that RES blocks TAC-induced cardiac hypertrophy through enhancing PTEN stability.

3.7. RES blocks immunoproteasome activity and expression leading to inhibition of PTEN degradation in vitro

To verify the effect of RES on cardiomyocyte hypertrophy and the underlying mechanism in vitro, we treated neonatal cardiomyocytes (NRCMs) with RES at a dose of 100 μ M, and found that it had no significant toxic effect on cardiomyocytes by TUNEL staining. Consistent with the findings in TAC-operated mice (Fig. 4E and D–F), RES treatment significantly reduced Ang II-induced increase of proteasome caspase-like, trypsin-like and chymotrypsin-like activities and the protein levels of β 1i, β 2i and β 5i in NRCMs compared with saline control (Fig. 7A–B). Accordingly, RES treatment reversed Ang II-induced decrease of PTEN ubiquitination (Fig. 7C) and protein level (Fig. 7D, lane 4 versus 3). These results indicate that RES can inhibit immunoproteasome activity and subunit expression leading to enhanced PTEN stability in vitro.

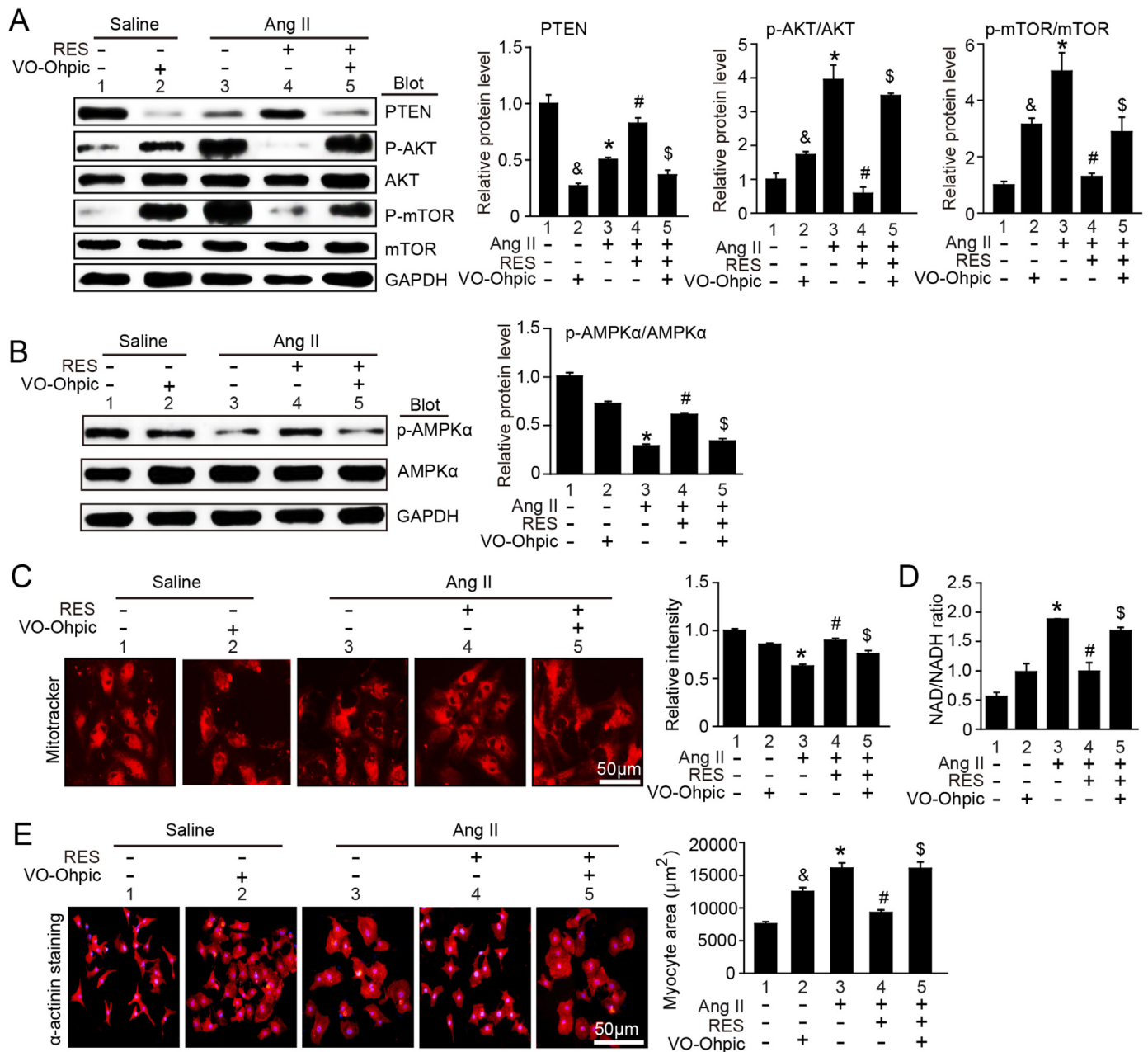


Fig. 8. RES inhibits cardiomyocyte hypertrophy through blocking hypertrophic signals and improving AMPK-mediated mitochondrial function in vitro. A–B, Representative immunoblotting analyses of PTEN, p-AKT, AKT, p-mTOR, mTOR, p-AMPKα and AMPKα in neonatal rat cardiomyocytes (NRCMs) treated with RES (100 μM) or vehicle with or without PTEN inhibitor VO-ohpic (5 μM) and then stimulated with Ang II (100 nm) for 24 h (n = 3, left). Quantification of the relative protein levels (right). GAPDH as an internal control. C, Analysis of mitochondrial membrane potential in NRCMs (left) with MitoTracker Red immunostaining (left), and quantification of the relative fluorescence intensity (right). D, NAD/NADH ratio. E, Representative images of double immunostaining (red for α-actinin, blue for DAPI) of NRCMs treated as D (left). Scale bar: 50 μm. Quantification of myocyte surface area. (150 cells counted per experiment; n = 3, right) *P < 0.05 versus saline; #P < 0.05 versus saline; \$P < 0.05 versus Ang II; &P < 0.05 versus Ang II.

3.8. Inhibition of PTEN abolishes protective effect of RES on cardiomyocyte hypertrophy in cultured cardiomyocytes

To test whether PTEN is involved in RES inhibitory effect on cardiomyocyte hypertrophy in vitro, we pretreated neonatal rat cardiomyocytes (NRCMs) with PTEN specific inhibitor VO-OHpic and then stimulated with Ang II (100 nm) for 24 h. Immunoblotting analysis showed that RES treatment markedly inhibited Ang II-induced degradation of PTEN, activation of AKT and mTOR and inactivation of AMPK (Fig. 8A–B, lane 4 versus 3), but this effect was reversed by VO-OHpic (Fig. 8A–B, lane 5 versus 4). Moreover, Ang II-induced decrease of mitochondrial membrane potential as indicated by staining with

MitoTracker Red and increase of NAD/NADH ratio and cardiomyocyte size were attenuated by RES (Fig. 8C–E, lane 4 versus 3), suggesting that RES improves Ang II-induced mitochondrial dysfunction. Conversely, this effect reversed by VO-OHpic (Fig. 8A–B, lane 5 versus 4). In addition, VO-OHpic treatment also reduced levels of PTEN, AMPK phosphorylation, mitochondrial membrane potential but induced activation of AKT/mTOR, increase of NAD/NADH ratio and cardiomyocyte size compared with vehicle control after saline treatment (Fig. 8A–E, lane 2 versus 1). Collectively, these results demonstrate that RES suppresses Ang II-induced cardiomyocyte hypertrophy through inhibiting degradation of PTEN by immunoproteasome in vitro.

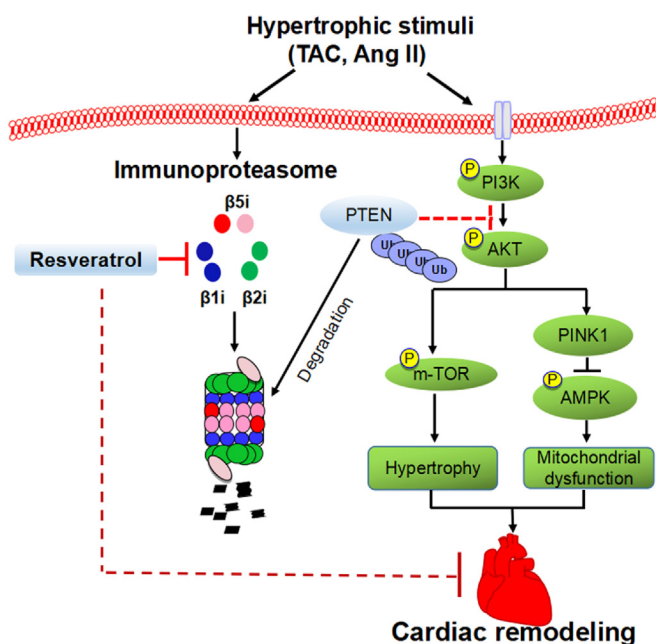


Fig. 9. A working model of RES-mediated cardioprotection in TAC-induced cardiac hypertrophy. Pressure overload induces upregulation of immunoproteasome activity and catalytic subunit expression, which in turn promotes degradation of PTEN thereby resulting in activation of AKT/mTOR and inhibition of AMPK pathways thereby leading to mitochondrial dysfunction, cardiac fibrosis, hypertrophy and dysfunction. In contrast, these effects were attenuated by inhibition of immunoproteasome by RES.

4. Discussion

The present results clearly elucidated a novel potential mechanism for RES connecting immunoproteasome, PTEN and the downstream signals (AKT/mTOR and AMPK) in the regulation of cardiac hypertrophic remodeling. Administration of RES significantly attenuated and reversed TAC-induced cardiac hypertrophic remodeling and dysfunction in mice. The inhibitory effect of RES on cardiomyocyte hypertrophy was confirmed *in vitro*. Mechanistically, RES inhibits immunoproteasome catalytic subunit ($\beta 1i$, $\beta 2i$ and $\beta 5i$) expression and activity, which blocked PTEN degradation and caused inhibition of AKT/mTOR and activation of AMPK thereby improving hypertrophic remodeling and dysfunction (Fig. 9). Hence, this study suggests that RES is a new inhibitor of the immunoproteasome, and may represent a promising therapeutic agent for treating hypertrophic diseases.

Sustained pressure overload induces cellular, molecular and morphologic changes in the heart, which contribute to maladaptive and progressive cardiac dysfunction and HF [1,2]. This response involves multiple mechanisms, including activation of neurohormonal system, cell apoptosis, oxidative stress, calcium handling and inflammation [1,2]. Although treatment of HF with angiotensin II receptor blockers, angiotensin converting enzyme inhibitors, diuretics and β -blockers, the mortality rate still remains high. Thus, it is essential to develop new therapeutic approaches for treating hypertrophy and HF. RES is a polyphenol compound that plays a critical role in improving cardiac hypertrophy and dysfunction in different hypertrophic models through multiple mechanisms [14,26,27,34,35]. In this study, we extended previous findings and discovered for the first time that RES prevented and reversed pressure overload-induced cardiac dysfunction and hypertrophic remodeling. This effect was associated with inhibition of immunoproteasome subunit expression and activity, which suppressed PTEN degradation leading to inactivation of AKT/mTOR and activation of AMPK.

The expression of immunoproteasome subunits is generally lower under basal conditions but can be induced for cells in response to

various stimuli, such as cytokines, heat shock and H_2O_2 [10]. Recent studies indicate that multiple hypertrophic stimuli such as Ang II, isoproterenol (ISO), high-salt and pressure overload also significantly upregulate expression and proteolytic activity of immunoproteasome in the heart [11,12,36,37], suggesting that increased expression of immunoproteasome subunits may play an important role in enhancing cardiac hypertrophic remodeling. Indeed, activation of standard or immunoproteasome is required for the development of cardiac hypertrophy and AF after Ang II, high salt, ISO or pressure overload [11,12,37,38]. In contrast, blocking proteasome activity by inhibitors such as PS-519, MG132, and epoxomicin remarkably attenuates or reverses cardiac fibrosis and hypertrophy induced by these stresses [36,37,39,40]. Moreover, some food-derived factors such as resveratrol, quercetin and δ -tocotrienol showed the ability to inhibit proteasome activity, which improves inflammation and atherosclerosis [41]. Here we presented first evidence that RES predominantly attenuated immunoproteasome catalytic subunits ($\beta 1i$, $\beta 2i$ and $\beta 5i$) and activity in TAC-treated hearts and Ang II-stimulated cardiomyocytes (Figs. 5 and 7). Thus, these results indicate that RES is a new inhibitor of immunoproteasome that may suppress PTEN degradation in cardiomyocytes.

PTEN has emerged as a critical regulator for PI3K/AKT/mTOR and PINK1-AMPK pathways involved in the governance of cardiac hypertrophy and dysfunction [7,8,42]. Cardiomyocyte-specific deletion of PTEN in mice results in activation of mTOR and suppression of autophagy and subsequent hypertrophic cardiomyopathy, while these effects are reversed by inhibition of mTOR by rapamycin [42]. Moreover, deletion of PTEN in cardiomyocytes inhibits activation of PINK1-AMPK signaling and autophagy leading to cardiac hypertrophy and dysfunction. Conversely, activation of AMPK by metformin rescued against PTEN deletion-induced these anomalies [8]. These data demonstrate an essential role for cardiomyocyte PTEN in maintaining cardiac homeostasis. Recently, our study showed that PTEN also inhibits atrial fibrosis via attenuating AKT and TGF- β /Smad2/3 signaling [12]. However, the signaling regulatory machineries in cardiac homeostasis remain elusive for PTEN. One possible pathway participating in PTEN signaling may be ubiquitin-mediated proteasomal degradation [9]. Indeed, several studies have shown that immunoproteasome subunits such as $\beta 1i$ and $\beta 2i$ are involved in regulation of PTEN protein level [12,43]. Knockout of $\beta 1i$ blocks PTEN degradation leading to inhibition of AKT activation in ischemic hearts [43]. Deletion of $\beta 2i$ also enhances PTEN stability leading to inhibition of AKT/IKK/NF- κ B signaling in atrial fibrillation (AF) [12]. In this study, we provide new evidence demonstrating that RES significantly reduced degradation of PTEN leading to AKT/mTOR inactivation, MAPK activation and inhibition of cardiac hypertrophy after Ang II or pressure overload. However, blocking of PTEN activity by VO-OHPic markedly reversed these effects (Figs. 1, 4 and 6). Together, these results indicate that RES inhibits cardiac hypertrophic remodeling through attenuation of PTEN degradation.

In summary, the present study for the first time demonstrated that RES treatment markedly ameliorates and reversed cardiac hypertrophic remodeling and dysfunction after pressure overload. Mechanistically, RES inhibited immunoproteasome, which blocked PTEN degradation leading to inhibition of AKT/mTOR and activation of AMPK pathways. Therefore, these findings suggest that RES is a novel inhibitor of immunoproteasome, and might be a novel therapeutic agent for treatment of cardiac hypertrophy and dysfunction. However, further studies are needed to elucidate the mechanism for RES to regulate the immunoproteasome subunit expression.

Acknowledgments

This work was supported by grants from China National Natural Science Funds (81330003 and 81630009), Dalian High-level Talents Innovation and Entrepreneurship Projects (2015R019), and Chang

Jiang Scholar Program (T2011160).

Declarations of interest

None.

Appendix A. Supplementary material

Supplementary data associated with this article can be found in the online version at doi:10.1016/j.redox.2018.10.021.

References

- [1] Y.K. Tham, B.C. Bernardo, J.Y. Ooi, K.L. Weeks, J.R. McMullen, Pathophysiology of cardiac hypertrophy and heart failure: signaling pathways and novel therapeutic targets, *Arch. Toxicol.* 89 (9) (2015) 1401–1438.
- [2] J. Heineke, J.D. Molkentin, Regulation of cardiac hypertrophy by intracellular signalling pathways, *Nat. Rev. Mol. Cell Biol.* 7 (8) (2006) 589–600.
- [3] T. Nagoshi, T. Matsui, T. Aoyama, A. Leri, P. Anversa, L. Li, W. Ogawa, F. del Monte, J.K. Gwathmey, L. Grazette, B.A. Hemmings, D.A. Kass, H.C. Champion, A. Rosenzweig, PI3K rescues the detrimental effects of chronic Akt activation in the heart during ischemia/reperfusion injury, *J. Clin. Investig.* 115 (8) (2005) 2128–2138.
- [4] G. Condorelli, A. Drusco, G. Stassi, A. Bellacosa, R. Roncarati, G. Iaccarino, M.A. Russo, Y. Gu, N. Dalton, C. Chung, M.V. Latronico, C. Napoli, J. Sadoshima, C.M. Croce, J. Ross Jr., Akt induces enhanced myocardial contractility and cell size in vivo in transgenic mice, *Proc. Natl. Acad. Sci. USA* 99 (19) (2002) 12333–12338.
- [5] P. Abeyrathna, Y. Su, The critical role of Akt in cardiovascular function, *Vasc. Pharmacol.* 74 (2015) 38–48.
- [6] R. Gelinas, F. Mailloux, J. Dontaine, L. Bultot, B. Demeulder, A. Ginion, E.P. Daskalopoulos, H. Esfahani, E. Dubois-Deruy, B. Lauzier, C. Gauthier, A.K. Olson, B. Bouchard, C. Des Rosiers, B. Viollet, K. Sakamoto, J.L. Balligand, J.L. Vanoverschelde, C. Beauloye, S. Hornam, L. Bertrand, AMPK activation counteracts cardiac hypertrophy by reducing O-GlcNAcylation, *Nat. Commun.* 9 (1) (2018) 374.
- [7] M.A. Crackower, G.Y. Oudit, I. Koziaradzki, R. Sarao, H. Sun, T. Sasaki, E. Hirsch, A. Suzuki, T. Shioi, J. Irie-Sasaki, R. Sah, H.Y. Cheng, V.O. Rybin, G. Lembo, L. Fratta, A.J. Oliveira-dos-Santos, J.L. Benovic, C.R. Kahn, S. Izumo, S.F. Steinberg, M.P. Wymann, P.H. Backx, J.M. Penninger, Regulation of myocardial contractility and cell size by distinct PI3K-PTEN signaling pathways, *Cell* 110 (6) (2002) 737–749.
- [8] N.D. Roe, X. Xu, M.R. Kandadi, N. Hu, J. Pang, M.C. Weiser-Evans, J. Ren, Targeted deletion of PTEN in cardiomyocytes renders cardiac contractile dysfunction through interruption of Pink1-AMPK signaling and autophagy, *Biochim. Biophys. Acta* 1852 (2) (2015) 290–298.
- [9] W. Wu, X. Wang, W. Zhang, W. Reed, J.M. Samet, Y.E. Whang, A.J. Ghio, Zinc-induced PTEN protein degradation through the proteasome pathway in human airway epithelial cells, *J. Biol. Chem.* 278 (30) (2003) 28258–28263.
- [10] A. Angeles, G. Fung, H. Luo, Immune and non-immune functions of the immunoproteasome, *Front. Biosci.* 17 (2012) 1904–1916.
- [11] W. Yan, H.L. Bi, L.X. Liu, N.N. Li, Y. Liu, J. Du, H.X. Wang, H.H. Li, Knockout of immunoproteasome subunit beta2i ameliorates cardiac fibrosis and inflammation in DOCA/Salt hypertensive mice, *Biochem. Biophys. Res. Commun.* 490 (2) (2017) 84–90.
- [12] J. Li, S. Wang, J. Bai, X.L. Yang, Y.L. Zhang, Y.L. Che, H.H. Li, Y.Z. Yang, Novel role for the immunoproteasome subunit PSMB10 in angiotensin II-induced atrial fibrillation in mice, *Hypertension* 71 (5) (2018) 866–876.
- [13] S. Wang, J. Li, J. Bai, J.M. Li, Y.L. Che, Q.Y. Lin, Y.L. Zhang, H.H. Li, The immunoproteasome subunit LMP10 mediates angiotensin II-induced retinopathy in mice, *Redox Biol.* 16 (2018) 129–138.
- [14] R.F. Guerrero, M.C. Garcia-Parrilla, B. Puertas, E. Cantos-Villar, Wine, resveratrol and health: a review, *Nat. Product Commun.* 4 (5) (2009) 635–658.
- [15] L.M. Hung, M.J. Su, W.K. Chu, C.W. Chiao, W.F. Chan, J.K. Chen, The protective effect of resveratrol on ischaemia-reperfusion injuries of rat hearts is correlated with antioxidant efficacy, *Br. J. Pharmacol.* 135 (7) (2002) 1627–1633.
- [16] M. Shen, G.L. Jia, Y.M. Wang, H. Ma, Cardioprotective effect of resveratrol pretreatment on myocardial ischemia-reperfusion induced injury in rats, *Vasc. Pharmacol.* 45 (2) (2006) 122–126.
- [17] W. Xuan, B. Wu, C. Chen, B. Chen, W. Zhang, D. Xu, J. Bin, Y. Liao, Resveratrol improves myocardial ischemia and ischemic heart failure in mice by antagonizing the detrimental effects of fractalkine*, *Crit. Care Med.* 40 (11) (2012) 3026–3033.
- [18] M.P. Robich, R.M. Osipov, R. Nezafat, J. Feng, R.T. Clements, C. Bianchi, M. Boodhwani, M.A. Coady, R.J. Laham, F.W. Sellke, Resveratrol improves myocardial perfusion in a swine model of hypercholesterolemia and chronic myocardial ischemia, *Circulation* 122 (11 Suppl.) (2010) S142–S149.
- [19] X. Cao, T. Luo, X. Luo, Z. Tang, Resveratrol prevents AngII-induced hypertension via AMPK activation and RhoA/ROCK suppression in mice, *Hypertens. Res.: Off. J. Jpn. Soc. Hypertens.* 37 (9) (2014) 803–810.
- [20] G.Q. Sun, Y.B. Li, B. Du, Y. Meng, Resveratrol via activation of AMPK lowers blood pressure in DOCA-salt hypertensive mice, *Clin. Exp. Hypertens.* 37 (8) (2015) 616–621.
- [21] V.W. Dolinsky, C.L. Soltys, K.J. Rogan, A.Y. Chan, J. Nagendran, S. Wang, J.R. Dyck, Resveratrol prevents pathological but not physiological cardiac hypertrophy, *J. Mol. Med.* 93 (4) (2015) 413–425.
- [22] I. Ahmet, H.J. Tae, E.G. Lakatta, M. Talan, Long-term low dose dietary resveratrol supplement reduces cardiovascular structural and functional deterioration in chronic heart failure in rats, *Can. J. Physiol. Pharmacol.* 95 (3) (2017) 268–274.
- [23] V.W. Dolinsky, A.Y. Chan, I. Robillard Frayne, P.E. Light, C. Des Rosiers, J.R. Dyck, Resveratrol prevents the prohypertrophic effects of oxidative stress on LKB1, *Circulation* 119 (12) (2009) 1643–1652.
- [24] H.H. Li, V. Kedar, C. Zhang, H. McDonough, R. Arya, D.Z. Wang, C. Patterson, Atrogin-1/muscle atrophy F-box inhibits calcineurin-dependent cardiac hypertrophy by participating in an SCF ubiquitin ligase complex, *J. Clin. Investig.* 114 (8) (2004) 1058–1071.
- [25] C. Kilkenny, W.J. Browne, I.C. Cuthill, M. Emerson, D.G. Altman, Improving bioscience research reporting: the ARRIVE guidelines for reporting animal research, *J. Pharmacol. Pharmacother.* 1 (2) (2010) 94–99.
- [26] X. Wang, H.X. Wang, Y.L. Li, C.C. Zhang, C.Y. Zhou, L. Wang, Y.L. Xia, J. Du, H.H. Li, MicroRNA Let-7i negatively regulates cardiac inflammation and fibrosis, *Hypertension* 66 (4) (2015) 776–785.
- [27] L. Wang, Y.L. Li, C.C. Zhang, W. Cui, X. Wang, Y. Xia, J. Du, H.H. Li, Inhibition of Toll-like receptor 2 reduces cardiac fibrosis by attenuating macrophage-mediated inflammation, *Cardiovasc. Res.* 101 (3) (2014) 383–392.
- [28] L. Wang, X.C. Zhao, W. Cui, Y.Q. Ma, H.L. Ren, X. Zhou, J. Fasset, Y.Z. Yang, Y. Chen, Y.L. Xia, J. Du, H.H. Li, Genetic and pharmacologic inhibition of the chemokine receptor CXCR2 prevents experimental hypertension and vascular dysfunction, *Circulation* 134 (18) (2016) 1353–1368.
- [29] J.M. Predmore, P. Wang, F. Davis, S. Bartolone, M.V. Westfall, D.B. Dyke, F. Pagani, S.R. Powell, S.M. Day, Ubiquitin proteasome dysfunction in human hypertrophic and dilated cardiomyopathies, *Circulation* 121 (8) (2010) 997–1004.
- [30] P.K. Mehta, K.K. Griendling, Angiotensin II cell signaling: physiological and pathological effects in the cardiovascular system, *Am. J. Physiol. Cell Physiol.* 292 (1) (2007) C82–C97.
- [31] P. Xie, S. Guo, Y. Fan, H. Zhang, D. Gu, H. Li, Atrogin-1/MAFbx enhances simulated ischemia/reperfusion-induced apoptosis in cardiomyocytes through degradation of MAPK phosphatase-1 and sustained JNK activation, *J. Biol. Chem.* 284 (9) (2009) 5488–5496.
- [32] F. Li, P. Xie, Y. Fan, H. Zhang, L. Zheng, D. Gu, C. Patterson, H. Li, C terminus of Hsc70-interacting protein promotes smooth muscle cell proliferation and survival through ubiquitin-mediated degradation of FoxO1, *J. Biol. Chem.* 284 (30) (2009) 20090–20098.
- [33] J. Zhang, Y. Choi, B. Mavromatis, A. Lichtenstein, W. Li, Preferential killing of PTEN-null myelomas by PI3K inhibitors through Akt pathway, *Oncogene* 22 (40) (2003) 6289–6295.
- [34] Z. Liu, Y. Song, X. Zhang, Z. Liu, W. Zhang, W. Mao, W. Wang, W. Cui, X. Zhang, X. Jia, N. Li, C. Han, C. Liu, Effects of trans-resveratrol on hypertension-induced cardiac hypertrophy using the partially nephrectomized rat model, *Clin. Exp. Pharmacol. Physiol.* 32 (12) (2005) 1049–1054.
- [35] P. Wojciechowski, D. Juric, X.L. Louis, S.J. Thandapilly, L. Yu, C. Taylor, T. Neticadan, Resveratrol arrests and regresses the development of pressure overload-but not volume overload-induced cardiac hypertrophy in rats, *J. Nutr.* 140 (5) (2010) 962–968.
- [36] N. Li, H.X. Wang, Q.Y. Han, W.J. Li, Y.L. Zhang, J. Du, Y.L. Xia, H.H. Li, Activation of the cardiac proteasome promotes angiotensin II-induced hypertrophy by down-regulation of ATRAP, *J. Mol. Cell. Cardiol.* 79 (2015) 303–314.
- [37] C. Depre, Q. Wang, L. Yan, N. Hedhli, P. Peter, L. Chen, C. Hong, L. Hittinger, B. Ghaleh, J. Sadoshima, D.E. Vatner, S.F. Vatner, K. Madura, Activation of the cardiac proteasome during pressure overload promotes ventricular hypertrophy, *Circulation* 114 (17) (2006) 1821–1828.
- [38] O. Drews, O. Tsukamoto, D. Liem, J. Streicher, Y. Wang, P. Ping, Differential regulation of proteasome function in isoproterenol-induced cardiac hypertrophy, *Circ. Res.* 107 (9) (2010) 1094–1101.
- [39] S. Meiners, B. Hoher, A. Weller, M. Laule, V. Stangl, C. Guenther, M. Godes, A. Mrozkiewicz, G. Baumann, K. Stangl, Downregulation of matrix metalloproteinases and collagens and suppression of cardiac fibrosis by inhibition of the proteasome, *Hypertension* 44 (4) (2004) 471–477.
- [40] W.E. Stansfield, R.H. Tang, N.C. Moss, A.S. Baldwin, M.S. Willis, C.H. Selzman, Proteasome inhibition promotes regression of left ventricular hypertrophy, *Am. J. Physiol. Heart Circ. Physiol.* 294 (2) (2008) H645–H650.
- [41] A.A. Qureshi, D.A. Khan, W. Mahjabeen, C.J. Pappasian, N. Qureshi, Nutritional supplement-5 with a combination of proteasome inhibitors (resveratrol, quercetin, delta-tocotrienol) modulate age-associated biomarkers and cardiovascular lipid parameters in human subjects, *J. Clin. Exp. Cardiol.* 4 (3) (2013).
- [42] X. Xu, N.D. Roe, M.C. Weiser-Evans, J. Ren, Inhibition of mammalian target of rapamycin with rapamycin reverses hypertrophic cardiomyopathy in mice with cardiomyocyte-specific knockout of PTEN, *Hypertension* 63 (4) (2014) 729–739.
- [43] Z.P. Cai, Z. Shen, L. Van Kaer, L.C. Becker, Ischemic preconditioning-induced cardioprotection is lost in mice with immunoproteasome subunit low molecular mass polypeptide-2 deficiency, *FASEB J.: Off. Publ. Fed. Am. Soc. Exp. Biol.* 22 (12) (2008) 4248–4257.